fire

MDPI

Article

Millennial-Scale Fire and Vegetation Change from a Rare Mid-Latitude Permafrost Fen (Beartooth Plateau, WY)

David B. McWethy *, Mio Alt and Anica Tipkemper-Wolfe

Department of Earth Sciences, Montana State University, Bozeman, MT 59717, USA; anica.tipkemperwolfe@student.montana.edu (A.T.-W.)
* Correspondence: dmcwethy@montana.edu

Abstract

Long-term fire histories are well-documented across most North American temperate forest systems, yet the fire regimes of high-alpine treeline environments remain poorly understood. Here, we present a millennial-scale fire history from the Sawtooth Fen Palsa (SFP), a rare permafrost fen palsa located in the high-alpine treeline ecotone of the Beartooth Plateau, Wyoming, a permafrost system now unraveling due to recent decades of rapid warming. Analysis of paleoenvironmental proxies from peat sediments overlying the permafrost reveals a multi-century peak in fire activity at the beginning of the record, ca. 10,000 cal yr BP, coinciding with the afforestation of newly deglaciated, ice-free sites. This initial surge in high-severity fire activity was followed by a decline when solar-orbitally driven increases in growing-season temperatures likely promoted forest opening and more surface fire activity within the SFP watershed. High-severity fire activity increased again during the mid-Holocene (ca. 5800–5000 cal yr BP), when effective moisture increased, favoring subalpine forest expansion and increased connectivity of woody biomass (sagebrush and forest), enhancing the potential for canopy fire spread. Only two small fire episodes were recorded in recent millennia when a rapid change in the sedimentation rate may indicate a partial loss of the sediment record. Rapid warming in recent decades has triggered the formation of dozens of thermal collapse ponds across the fen palsa. The frequency of these features has more than doubled since 2000 CE, underscoring the degradation of underlying permafrost in response to changing climatic conditions. Continued warming is expected to cause the complete loss of the permafrost lens and alter ecosystem dynamics, disturbance regimes, and carbon and nutrient cycling in alpine systems throughout the Rocky Mountains.

Keywords: fire; palsa; fen palsa; permafrost; US Rocky Mountains; alpine; alpine fires; permafrost degradation

Check for updates

Academic Editor: Jai Garg

Received: 27 December 2025
Revised: 14 February 2026
Accepted: 18 February 2026
Published: 26 February 2026

Copyright: © 2026 by the authors. Licensee MDPI, Basel, Switzerland. This article is an open access article distributed under the terms and conditions of the Creative Commons Attribution (CC BY) license.

1. Introduction

1.1. The Vulnerability of High-Elevation Ecosystems

Ecosystems throughout the western United States are responding to rapid warming, with higher-latitude alpine environments warming at greater rates than lowland environments [1,2]. These high-elevation systems serve as critical sentinels for climate change, yet their long-term ecological baselines are often obscured by a lack of paleoenvironmental data. Ecosystem models predict latitudinal and altitudinal shifts in forest systems in response to warming temperatures [3,4], though local site conditions play an important role in influencing the directional outcomes [5]. For example, while rising isotherms typically

drive upward tree migration, subalpine forests could become moisture-limited rather than exhibiting an expected positive growth and recruitment response to continued warming temperatures [6,7].

The current rate of climatic change driving ecosystems at high elevations towards possible extinction events related to mountaintop traps highlights a need to better understand the magnitude of paleoclimatic and paleoecological changes in the subalpine treeline [8]. Species adapted to the uppermost limits of alpine systems face greater risks, as mountain-top elevations limit the upper range of climatic envelopes that support their suitable habitat. Additionally, records focusing on how subalpine treeline position and species composition have fluctuated across multiple timescales are needed to clarify how changes in fuel conditions can lead to novel fire regimes in high-elevation systems. Disentangling these drivers is essential for forecasting future fire risk, as the controls of temperature and moisture on fuel aridity and fuel connectivity in alpine systems are often decoupled from adjacent lowland systems [9].

While the vegetational history of the Greater Yellowstone Ecosystem (GYE) since the last glacial period has been studied extensively through the analysis of pollen, charcoal, and other proxies from lakes and wetlands [10–14], there are few records of fire activity and environmental change from high-elevation alpine ecosystems at the subalpine forest treeline to alpine tundra ecotone [7,15,16]. This gap is particularly evident in relation to the interaction between fire and permafrost features, where fire is typically thought to be limited or absent [16].

1.2. Alpine Permafrost, Palsa Dynamics and Changing Fire Regimes

Alpine permafrost features are relatively rare features in the contiguous US, with undocumented estimates of ca. 100,000 km^2 in alpine settings in the western US [17], within the Rocky Mountain cordillera. Permafrost landscapes support unique high-elevation peatlands, including bogs and fens, and function as important reservoirs of carbon and methane. However, warming temperatures are extending the latitudinal and elevational extent of permafrost degradation of alpine permafrost that occur in the coterminous western United States [18].

Fen palsas, peat-covered permafrost mounds that form within wetland basins underlain by permafrost, are even rarer landforms commonly associated with the subarctic and subalpine permafrost systems at higher latitudes (>50° N) [18,19]. The Sawtooth fen palsa is the only fen palsa documented in the contiguous US [19], likely because their formation and persistence require a combination of climatological conditions that more typically occur at higher latitudes. These conditions include cold, dry continental climates with 500–1500 thawing degree days (sum of daily mean temperature above 0 °C totaled over a year), 500–4000 freezing degree days (sum of the daily mean temperature below the freezing point 0 °C totaled over a year), around 300 mm of rainfall, and high soil moisture accumulation [20].

Following several decades of rapidly warming temperatures and the reduced frequency of freezing degree days and cold, dry conditions, permafrost features are unraveling throughout North America [18]. Since ~2000 CE, permafrost degradation threatens to destabilize many of the fen-palsa systems, with significant implications for alpine ecosystems, disturbance regimes, and carbon cycling. Fire activity in these cold, high-elevation settings with short fire seasons was thought to be low except during centennial- to millennial-scale climate-driven warm periods [7,16].

Historical fire activity is poorly documented in fen palsa systems, particularly at lower latitudes, although changes in fire regimes under a warming climate in high-latitude permafrost systems are well-documented [21–23]. Persistent warming in permafrost systems

can initiate a self-reinforcing feedback in which the active layer thickness increases and surface fuel drying promotes fire spread when ignitions occur. Although fire-induced active-layer deepening is typically more pronounced in forested permafrost systems, slow-moving smoldering fires in treeless peatlands can consume dry peat and remove the insulating layer that protects underlying permafrost [21,24]. Post-fire processes may further accelerate instability because drying peatlands promote fuel accumulation, sometimes including woody fuels, which can intensify subsequent fires under continued warming [21,22]. Permafrost thaw and associated changes in fire activity are therefore producing cascading ecosystem effects, with significant consequences for carbon storage, nutrient cycling, and hydrology [25].

1.3. Research Objectives

Here, we investigate the long-term environmental change and fire history of a high-alpine wetland area by analyzing pollen and charcoal from a rare mid-latitude c. 8-hectare alpine fen palsa, the Sawtooth Fen Palsa (SFP), located at c. 2950 masl on the high-alpine Beartooth Plateau, Wyoming. First identified in 1961 [26], the SFP is characterized by an underlying 0.5–2.0 m thick permafrost lens that has been melting due to recent decades of rapid warming. This has resulted in the instability of the fen palsa, with the desiccation of several meters of peat overlaying sections of permafrost causing a shift from a stable fen palsa mound to a matrix of thaw depression ponds interspersed by pillars of dried peat. The number of depression ponds has been increasing in number since the late 20th century [27].

Using a multiproxy comparison, we evaluate past fire activity (macroscopic charcoal influx), vegetation change (pollen), and climatic conditions (lithology, sedimentation rates) to reconstruct a long-term record of fire activity and environmental change at a unique alpine fen palsa in the Northern Rocky Mountains to address the following questions: (1) How stable was this low-latitude permafrost feature throughout the Holocene? (2) What was the frequency and character of fire activity at this alpine site? (3) How did vegetation respond to changes in fire activity? (4) How is this SFP changing in response to recent decades of warming?

This paleoenvironmental record offers a rare, long-term perspective on alpine fire–climate–permafrost interactions, and understanding these dynamics is essential for anticipating ecosystem shifts under continued warming.

2. Materials and Methods

2.1. Study Site Description

The Beartooth Mountain Range in south-central Montana and northwest Wyoming is the highest mountain range in the state of Montana (3904 masl at its highest point, Granite Peak). The mountain range lies within the Custer, Gallatin, and Shoshone National Forests. The vegetation zonation along the elevation gradient includes *Pinus contorta* (lodgepole pine) and *Pseudotsuga menziesii* (Douglas fir) forests at lower elevations, subalpine forests of *Picea engelmannii* (Engelmann spruce), *Abies lasiocarpa* (subalpine fir), and *Pinus albicaulis* (whitebark pine), and alpine tundra vegetation dominates above approximately 3000 masl, characterized by Poaceae (grass), *Carex* (sedge), *Salix* (willow), and other herbaceous vegetation [27].

The climatology of the Beartooth Plateau is governed by large-scale atmospheric circulation patterns: most precipitation is received during the cool season (October–April) from westerly storm tracks originating over the Pacific Ocean, and a secondary spring (April–June) precipitation pulse can deliver substantial moisture to the region and typically occurs due to regional recycling of winter moisture and upsloping easterlies laden with

plains moisture that may extend from as far away as the Gulf of Mexico [28]. These spring precipitation events can occur as convectional storms or snowfall at high elevations. The late summer season is typically dry due to the presence of the Pacific subtropical high-pressure system, which redirects moisture away from the Northern Rocky Mountains [29].

The SFP (44°53′32.54 N, 109°27′34.82 W) is located in a glacially carved basin south of Sawtooth Peak along the Beartooth Uplift in Wyoming (Figure 1). This is thought to be the southernmost palsa feature in North America, over 1000 km south of the closest known fen palsa in Canada [19]. A survey of the SFP in 1961 reported the depth to permafrost as approximately 38–46 cm [26].

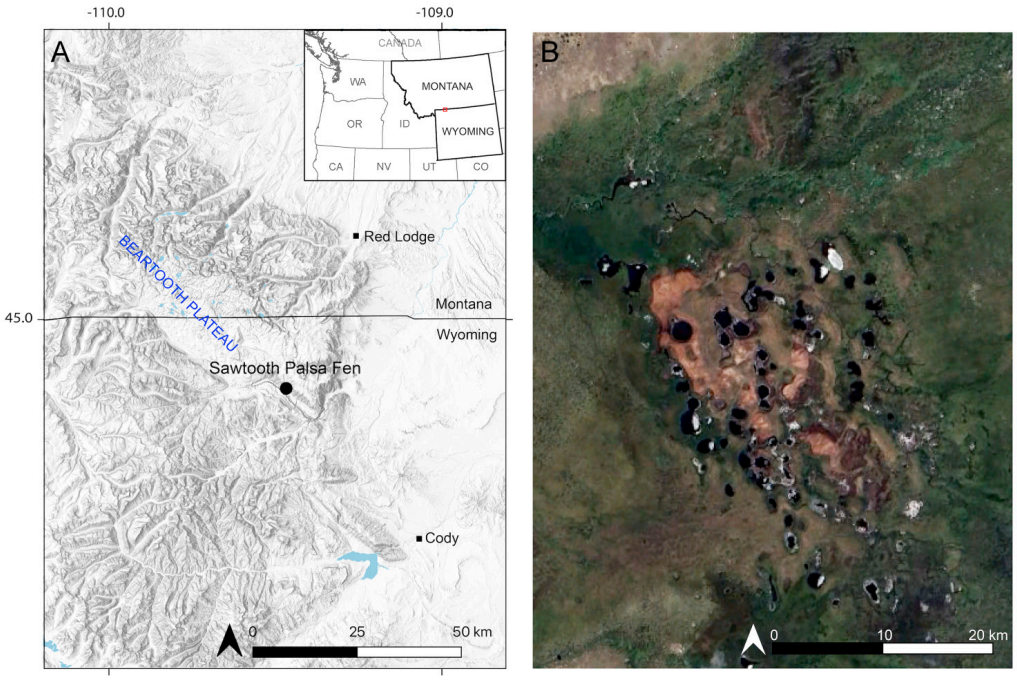


Figure 1. Regional map showing the location of the Sawtooth Fen Palsa, Beartooth Uplift, Wyoming (**A**). Satellite image of the SFP with thermal depression ponds (**B**) (2023 Google Earth Airbus satellite image, accessed September 2025).

The SFP vegetation is primarily composed of grasses (*Festuca brachyphylla*, *Deschampsia caespitosa*, *Agrostis mertensii*), sedges (*Carex scopulorum*, *C. canescens*, *C. aquatilis*), herbs (*Rumex paucifolius*, *Antennaria lanata*), and a mix of mosses [27]. The basin surrounding the palsa consists of sedges (*Carex scopulorum*, *C. praeceptorum*, *C. illota*, and *C. aquatilis*), grasses (*Deschampsia caespitosa*), small shrubs (*Salix planifolia*, *Rosa woodsii*), and herbaceous plants typical of alpine tundra (*Artemisia scopulorum*, *Carex* sp., *Geum rossii*, *Phlox caespitosa*, *Polygonum bistortoides*, *Potentilla diversifolia*, *Gentiana algida*, *Phyllodoce empetriformis*) across the broader Beartooth alpine ecosystem [27]. The treeline ecotone in this basin is diffuse with an approximate upper elevation of ~3060 m asl, about 0.3 km from SFP. The closest dense subalpine forest stand of whitebark pine and Engelmann spruce is located ~0.5 km away at ~3000 m asl.

Interpolated climate normals for 1991–2020 (PRISM Climate Group, 2022) indicate the basin receives an average of ~800 mm of annual precipitation. Most precipitation is received in the winter and spring months as snow (DJF = 175 mm, MAM = 275 mm), and the least in the summer months (JJA = 165 mm). Temperatures are highest in July (average of 12 °C), and lowest in December (average of −9.5 °C). The average annual temperature is −0.1 °C.

2.2. Lithology, Sediment Sampling, and Chronology

Our 2022 surveys of the depth to permafrost varied from 30 cm to nearly 200 cm at different locations on top of the palsa dome, indicating the peat depths above the permafrost vary. We cored a location where sediments overlaying the permafrost surface were approximately 150 cm. Peat sediments were collected using a D-section peat coring device, which is designed to retrieve soft sediments without significant compression or distortion of the stratigraphy. Three sediment cores, each 50 cm in depth (150 cm length in total), were retrieved in the field. The cores were wrapped in plastic wrap, secured in split-PVC tubes, and stored in cold storage at Montana State University for analysis. The last 50 cm sediment core interfaced with the beginning of the permafrost layer at ~150 cm in total depth. Thus, the 150 cm of sediment was bounded and underlain by a permafrost layer.

In the laboratory, the lithology of the SFP cores was described based on visual inspection of color (Munsell), grain size, and organic content. Nine bulk sediment samples spanning the three cores were submitted to the NOSAMS Woods Hole Oceanographic Institute for Accelerator Mass Spectrometry (AMS) radiocarbon dating (Table S1). Two macrofossils found within the top 4 cm of the permafrost layer, at the boundary of the peat sediments and the surface of the permafrost, were also radiocarbon dated to constrain the onset of peat accumulation above the permafrost. The AMS radiocarbon ages were converted to calibrated ages using CALIB Radiocarbon Calibration Program 8.2 [30].

To develop a robust chronology for the sediment record, an age–depth model for the SFP was created using BACON program [31] (Figure 2). BACON utilizes a Bayesian statistical approach to reconstruct accumulation rates. This method uses millions of Markov Chain Monte Carlo (MCMC) iterations to estimate age–depth relationships, accommodating the variable sedimentation rates typical of dynamic peatland environments.

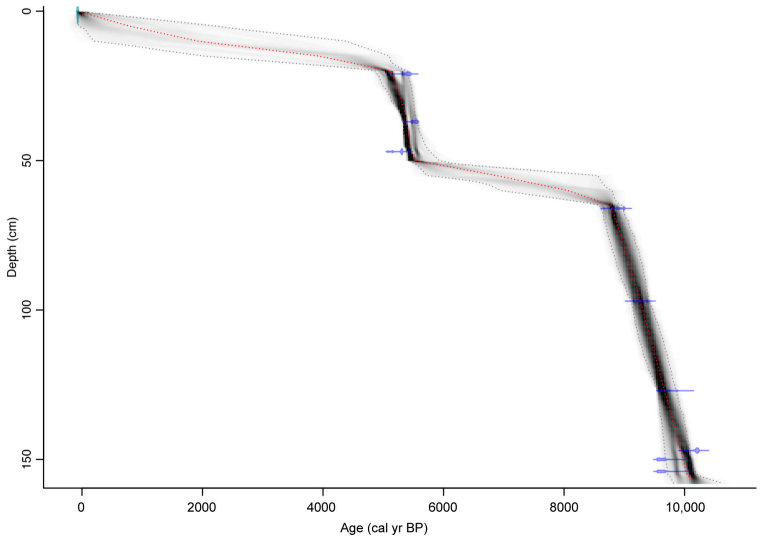


Figure 2. Age–depth diagram and lithology of the Sawtooth Fen Palsa cores. The age–depth model derived from the BACON program [31] used nine radiocarbon dated macrofossils and bulk sediments from the SFP sediments (Table S1). The red dotted line is the median probability age for each depth, and the black dotted lines indicate the 95% probability range. Calibrated dates and modeled calibrated probability distributions detailed in Table S1.

2.3. Pollen Analysis

The SFP sediments were processed for pollen following the standard procedures of Bennett and Willis [32]. Sediment samples of 1 cm^3 were taken at regular intervals and treated with hydrochloric acid (HCl) to remove carbonates, potassium hydroxide (KOH) to

digest humic acids, hydrofluoric acid to remove silicates, and acetolysis to remove cellulose. A tablet with a known concentration of *Lycopodium* spores was added to each sample prior to chemical processing to calculate pollen concentration (grains/cm^3) and accumulation rates (grains $cm^{-2}yr^{-1}$).

A minimum of 300 pollen grains were counted per sample at 400–1000x magnification and identified to the lowest possible taxonomic level using reference collections at Montana State University and pollen manuals [33–35]. Pollen results were separated into stratigraphic zones designated through cluster analysis performed by the CONISS program, which uses a stratigraphically constrained incremental sum of squares method to identify significant changes in assemblages [36]. Tree species and several upland herb species that were present in very small percentages were grouped together in "other trees" and "other shrubs and herbs" categories.

2.4. Charcoal Analysis

Fire history was reconstructed using macroscopic charcoal analysis. Contiguous sediment samples of 2 cm^3 were taken at 1 cm intervals throughout the SFP cores. These samples were processed following the procedures outlined by Whitlock and Larsen [37]. Samples were soaked in a deflocculant and washed through a 125 µm sieve. Charred particles retained on the sieve (>125 µm) were counted under a stereomicroscope. This size fraction has been shown to represent local-to-watershed scale fire events, as larger particles do not travel far from the source of combustion [38].

Charcoal counts were converted to charcoal accumulation rates (CHAR, particles cm^{-2} yr^{-1}) using the sedimentation rates derived from the age–depth model. Fire events and changes in fire frequency over time were identified using the CharAnalysis software for MatLab [39]. Background charcoal accumulation rates (BCHAR), which represent the regional charcoal pool and secondary depositional processes, were calculated using a 500-year Lowess smoother. This window width was selected to optimize the signal-to-noise ratio, effectively separating local fire peaks from the background noise. Peaks exceeding a locally defined threshold were identified as fire episodes (i.e., one-to-several fire events occurring within sample peaks).

3. Results

3.1. Lithology and Chronology

Sediment lithology for each of the three 50 cm length cores consisted of sedge peats within an organic fine-grained sediment matrix. There were no distinct changes in lithology or grain size across the three cores. The age–depth chronology indicates the peat sequence spans ca. 10,250 cal yrs BP (Figure 2). Radiocarbon-dated macrofossils found within the permafrost ice lens indicate the boundary layer between the peat sediments and the surface of the permafrost ice occurs in this same time interval, ca. 10,000 cal yr BP. This confirms that the permafrost feature established after deglaciation and has persisted throughout the Holocene.

The interpolated age–depth chronology derived from BACON shows several distinct changes in sedimentation rate (sediment deposited per year cm/yr^{-1}). The sedimentation rate is relatively rapid (>0.05 cm/yr^{-1}) from ca. 10,250–8500 and ca. 5800–4700 cal yr BP. Conversely, sedimentation rate is relatively slow (<0.01 cm/yr^{-1}) from ca. 8500–5800 cal yr BP and ca. 4970 cal yr BP—to present day. Changes in the sedimentation rate did not correlate with visible changes in sediment color, grain size, or organic material. The consumption or loss of sediments (via fire or erosion) during these intervals of slow sedimentation may explain the absence of noticeable lithological changes.

3.2. Fire Activity

Analysis of macroscopic charcoal influx (charcoal particles cm^2/yr^{-1}) as a proxy for past fire activity/woody biomass burning suggests the SFP experienced high-severity fires at different periods of the Holocene. A pronounced decrease in the rate of sediment/peat deposition and hiatuses in sediment/peat deposition indicate climatic and environmental conditions at the fen palsa led to loss of some part of the paleoenvironmental record via erosive processes or consumption by fire (Figure 3).

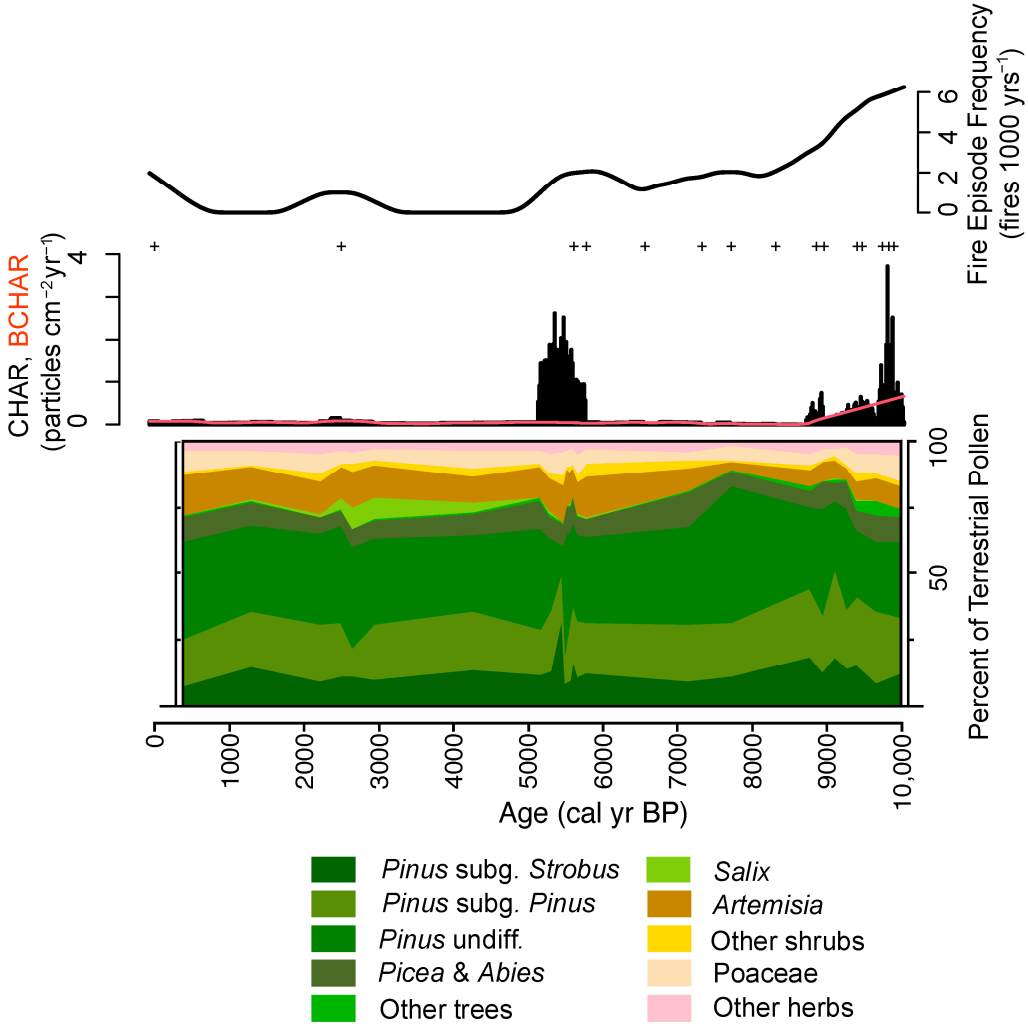


Figure 3. Standardized charcoal influx over the period of the record for the Sawtooth Fen Palsa (top panel, black bars) with fire frequency (black line, fires per 1000 yrs) and records of fire episodes (95% threshold) for the Sawtooth Fen Palsa (+ symbols represent one statistically significant fire peak). Background charcoal influx Lowess smoother (red line) used for identifying 95% peak events from CharAnalysis [39]. Significant fire peaks (+ signs) likely represent stand replacing fire episodes in forest/shrub vegetation. Fire-episode frequency is the number of peaks smoothed over a 1000-year moving window. Relative percent change in dominant terrestrial arboreal, shrub and herbaceous pollen (percent of the total terrestrial pollen sum) (bottom panel).

Early Holocene (ca. 10,250–7500) Fire Activity: Fire activity and biomass burning of woody vegetation was high during the beginning of the early Holocene. During this period, CHAR consistently exceeded two particles cm^2/yr^{-1}, and seven high-severity fire events were recorded.

Mid-Holocene (ca. 7500–5000) Transition: After a decline in peak fire events ca. 8500 yrs ago, low levels of charcoal influx persisted. Increased seasonality and warmer

summer conditions could have led to drying of the peat surface and loss of charcoal through surface fire, or erosive processes that consumed or removed charcoal from the record. Peat accumulation increased near the end of the mid-Holocene (ca. 5800–5000 cal yr BP), recording another period of high fire activity (CHAR > 2 particles cm^2/yr^{-1}). This period of high woody biomass burning coincides with increases in winter/spring temperatures recorded by adjacent sites [6,35–37].

Late-Holocene (ca. 5000-present) Absence of Fire Activity: The late Holocene fire record indicates minimal biomass burning at the fen palsa. Two fires were recorded at ca. 2900 cal yr BP and ca. 200 cal yr BP. The initial onset of this decline in fire activity parallels the onset of cool and wet climatic conditions at adjacent high-alpine settings when snow and ice cover increased year-round at high elevations of the Beartooth Plateau [6,40]. The pronounced decrease in late-Holocene peat accumulation suggests that much of the record of biomass burning following ca. 2900 cal yr BP was likely removed by erosive processes (aeolian or water) or consumed by fire.

3.3. Vegetation Change

Pollen data indicate that for millennia the SFP basin was dominated by sedges and grasses with surrounding uplands dominated by sagebrush, forbs, and forests of pine, spruce, and fir (Figures 3 and 4).

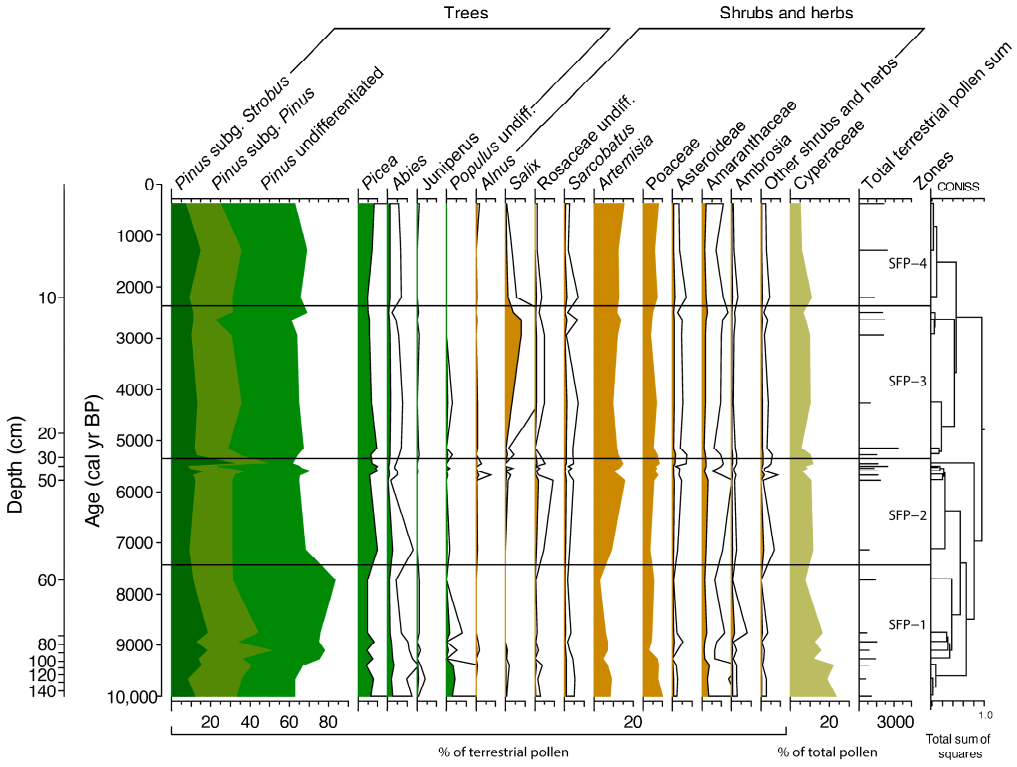


Figure 4. Pollen percent data for select plant taxa from the SFP sediments. Terrestrial pollen percentages based on terrestrial pollen sums. Cyperaceae based on aquatic pollen sums.

Early Holocene (ca. 10,250-c. 7500): Pollen percentages of Cyperaceae (sedges) were highest (18–23%) from ca. 10,250–9400 cal yr BP and then decreased (to 7%) by ca. 7500 cal yr BP, suggesting hydrologic conditions supported extensive sedge wetlands during the early Holocene. Poaceae and Amaranthaceae levels were also high, reflective of the surrounding open basin. *Pinus* levels were moderate (62–66%) between ca. 10,250–9000 cal yr BP, then increased to the highest levels of the record (75–83%) between ca. 9000–7500 cal yr BP. *Picea* and *Abies* levels were also moderate (6 and 2%,

respectively), and *Populus* levels were highest (2–4%) at the base of the core from ca. 10,250–9000 cal yr BP. This suggests pine/spruce/fir/aspen parklands and open forests likely established along the uplands surrounding the wetland from ca. 10,250–9000 cal yr BP. Higher pollen percentages of *Pinus* (subgenus *Strobus* type) between ca. 9000–7500 cal yr BP indicate forest densification of what is likely pollen from whitebark pine.

Mid-Holocene (ca. 7500–5000 cal yr BP): Artemisia increased during the mid-Holocene (from 8 to 14%), at the expense of *Pinus* (back down to 64%), although *Picea* and *Abies* pollen levels increased (6–10% and <1–3%, respectively). Cyperaceae also remained at lower levels, likely due to a contraction in the wetland margin extent.

Late Holocene (ca. 5000–2500 cal yr BP): Pollen percentages of *Pinus* subg. *Strobus* show a distinct peak ca. 5500 cal yr BP (35%), then return to moderate levels (11–13%). Other than the spike in *Pinus* subg. *Strobus*, total *Pinus*, *Picea,* and *Abies* remained consistent (60–68%, 5–9%, 4–2%, respectively). Following this, sediment accumulation rates slow, or possibly cease completely, ca. 5000 cal yr BP–present day indicating the loss of the top of the sediment core, or climatic conditions (cold temperatures or possibly ice accumulation) prevented the accumulation of organic materials. During this decline in sediment accumulation, *Salix* pollen increased (to 8%), and Poaceae and *Artemisia* levels remained moderate (9–13%, 3–7%, respectively).

Late Holocene/Modern (ca. 2500 cal yr BP—present day): Pollen percentages remain relatively stable and consistent with the previous zone for the last two millennia, other than a decrease in *Salix* (to 0%), and decrease in Cyperaceae (from 10 to 5%).

4. Discussion

The few high-elevation long-term records of fire and vegetation change from the US Rocky Mountains provide important insights into alpine ecosystem dynamics, upslope and downslope shifts in treeline, and the ecological response to changes in fire activity [4,6,7,41]. This fire and vegetation history from the only known fen palsa in the lower latitudes of North America [19] suggests high-severity canopy fires were a common occurrence at high elevations during the early- and mid-Holocene. Rapid changes in sedimentation also indicate the SFP experienced periods of instability leading to the loss of peat layers overlying the palsa dome. Recent warming is leading to an unraveling of the permafrost underlying the fen system, likely signaling a change in fuel conditions that will promote increased fire activity and changing carbon dynamics in coming decades.

4.1. Early Holocene Fire Regimes

The SFP experienced several high-severity fire events during the early Holocene, when spruce, fir, aspen, and grasses dominated the high-alpine environment (Figures 3–5). These early Holocene fires and high-elevation spruce and fir forests coincide with regional records showing the upwards expansion of forests in the alpine environments of the Northern Rocky Mountains [6,7,41–43]. This synchrony in increased fire activity across the region was likely in response to climate variability driven by changes in solar orbital forcing (high summer insolation), which created drier and warmer summers but cooler winters. These conditions allowed woody biomass to expand to high elevations, while simultaneously drying fuels sufficiently during the summer fire season to facilitate canopy fire spread. The SFP record suggests that, however sparse, the treeline forests surrounding the fen palsa burned readily once vegetation was established and seasonal conditions led to adequate fuel drying.

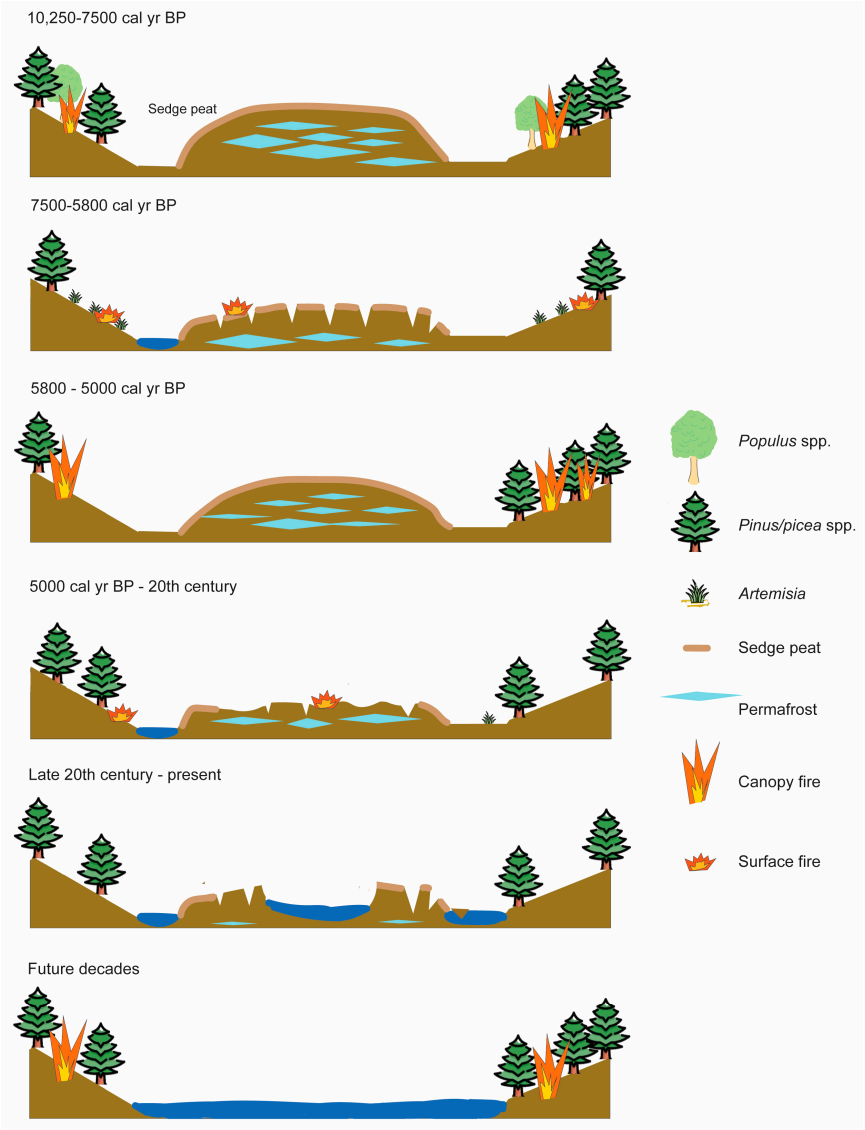


Figure 5. Depiction of key intervals revealing shifts in SFP fire regimes and ecosystem change. Early Holocene ca. 10,250–7500 cal yr BP: High-severity fires accompanied afforestation of deglaciated alpine zones and upward migration of treeline with the expansion of spruce, fir and aspen forests surrounding the SFP. Early- to mid-Holocene ca. 7500–5800 cal yr BP: Warm, dry conditions led to an increase in sagebrush, more open, fragmented forests and reduced woody fuels that likely supported low-severity surface fires after ca. 7500 cal yr BP that may have consumed surface peats removing part of the sediment record. Mid-Holocene warm interval ca. 5800–5000 cal yr BP: Peat accumulation rates rose, recording a period of high-severity fire activity as effective moisture increased along the plateau. Late Holocene ca. 5000 cal yr BP to 20th century: Slow sedimentation rates highlight possible instability of the SFP surface and associated loss of peat sediments through desiccation, consumption by surface fires or erosion. Late 20th Century to present: Warming temperatures and a decrease in freezing degree days, soil moisture, and generally warmer temperatures resulted in the unraveling of the permafrost underlying the fen system. Future decades: Drying of peat and soils within an ever-expanding thaw depression pond matrix eventually leads to the loss of the SFP. Warming conditions lead to persistently dry fuels during an expanding fire season promoting fire spread in upland forest patches surrounding the SFP basin.

4.2. The Mid-Holocene Shift and the Whitebark Pine Anomaly

Macroscopic charcoal influx declines ca. 8500–5800 cal yr BP, coinciding with a pronounced reduction in the sedimentation rate, suggesting a period of aridity that resulted in slow peat accumulation, if not the total desiccation of the peat surface and subsequent

loss of surface peat (and therefore charcoal) due to degradation, erosion, or fire, which may also have consumed the peat surface. Continued warm, dry summers due to high seasonality likely facilitated the occurrence of fires during this period [41], yet colder winters may have shortened the fire season, and less dense forest and fewer connected canopy fuels after 7000 cal yr BP likely prevented the generation of large charcoal peaks typical of stand-replacing events. The possible loss of the part of the fire record obscures a complete record of fire activity during this interval.

As rapid peat/sediment accumulation resumed, charcoal influx increased, indicating high-severity fires occurred for several centuries (ca. 5800–5000 cal yr BP). We interpret this increase in fire activity forested uplands surrounding the SFP to be related to a pronounced period of warming evident in adjacent climate records [40]. An increase in *Pinus strobus* type pollen (likely *Pinus albicaulis*—whitebark pine) during this interval suggests whitebark pine benefited from increased fire activity. Under certain fire severities and frequencies, whitebark pine trees can confer an advantage over subalpine arboreal competitors as fires reset succession, allowing whitebark pine seedlings to establish in open sites following fires [44]. The increase in whitebark pine pollen coincides with other records suggesting the upward movement and establishment of whitebark pine stands across the Beartooth Plateau [6,7].

4.3. Late-Holocene Cooling and Hiatus in Peat Accumulation

Only two small fires (low peak magnitude fire events) were recorded from when seasonality decreased, summers became cooler and wetter, and alpine glaciers began re-advancing in northern Montana ca. 4000–2000 cal yr BP [45]. A pronounced decline in peat accumulation occurred during this period, coinciding with cooler climatic conditions [6,40,41]. The initial decline or hiatus in accumulation could be related to a general decline in primary productivity and delivery of organic material into the SFP due to cooler conditions. Alternatively, a substantial increase in the accumulation of snow and ice recorded at nearby sites at similar elevations after ca. 4000–3000 cal yr BP could indicate the fen palsa was covered by snow and ice for much of the year, restricting the accumulation of organic sediments and preventing fire activity within the watershed [6,7,40].

After ca. 3000 cal yr BP, the pronounced slowdown in peat accumulation likely indicates the top peat layers were lost to desiccation, degradation, erosive processes, or that the surface peats were consumed by fire. High-magnitude oscillations between wet and dry periods and extended droughts such as the Medieval Climate Anomaly (ca. 1000–750 cal yrs BP) [46] could have led to fires that consumed desiccated peat surface or desiccation alone, provided conditions whereby aeolian or water erosion could have removed any record of fire and paleoenvironmental change for the last several millennia.

4.4. Modern Fen Palsa Dynamics and Degradation

While small permafrost features have been identified across high-elevation systems throughout North America, fen palsas are rare features more commonly associated with permafrost zones at higher latitudes (>50° N). Climatic conditions supporting the development and persistence of fen palsas are declining. Warmer temperatures, decreasing number of freezing days, and drying soils are driving a rapid collapse of permafrost features, especially in the discontinuous permafrost zone and alpine permafrost features at lower latitudes. These changes are occurring in the high alpines of the US Rocky Mountains as evidenced by the rapid melting of persistent ice patches and small permafrost wetlands [6,40]. Recent decades of warming and subsequent permafrost degradation have destabilized the SFP system; and with continued warming, the SFP permafrost lens will likely disappear.

Images show a more than double-fold increase in the number of thermal depression ponds at the SFP basin between 1994 and 2022 [19] (Figure 6A,B). A field survey of the SFP in 1982 notes the presence of raised peat deposits and a small number of thermal depression ponds and polygonal cracking of the fen palsa surface peats resulting from freeze–thaw dynamics, but images from this survey depict a largely intact palsa system, contrasting sharply with the system's current instability.

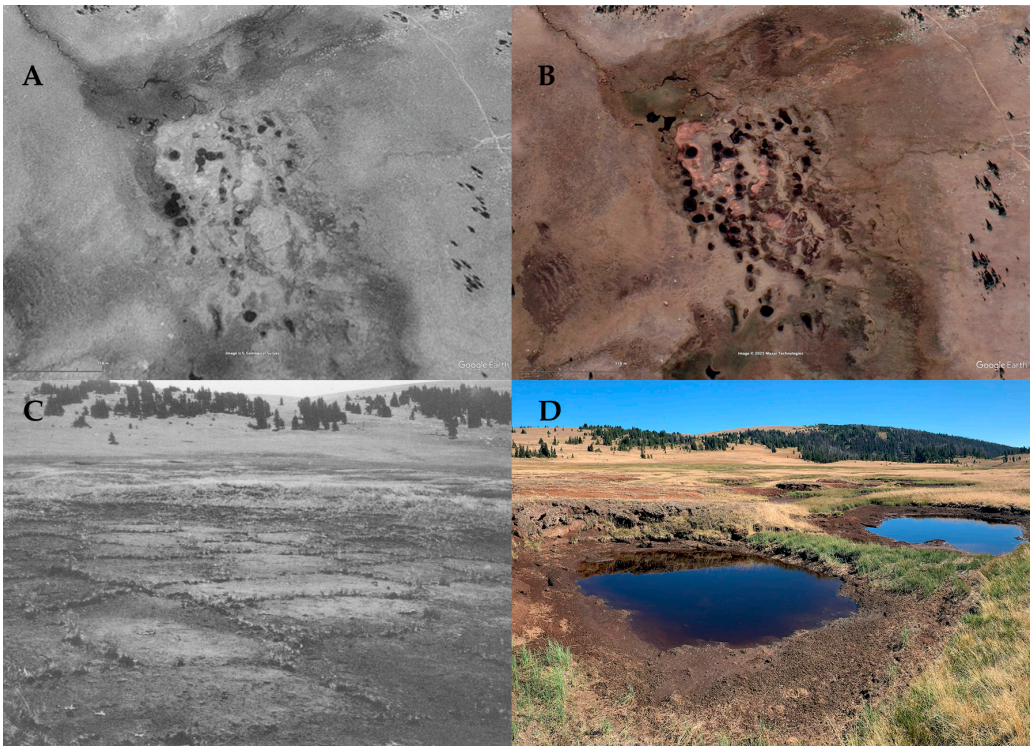


Figure 6. Images showing change in the abundance of thermal depression ponds between August 1994 (**A**), USGS aerial photo and September 2022 (**B**), Google Earth Airbus satellite image (Google Earth, accessed September 2025). The number of thermal depression pond features more than doubled over the 28-year period. Bottom panel shows images from 1982 to 2022 (**C**,**D**) from the same vantage point looking north. Image from Collins et al. 1984 [19] taken in 1982 (**C**) shows polygonal frost cracks across intact surface elevation of SFP contrasting with the unraveling of the peat surface following the development of several thermal collapse ponds in the bottom right image taken in 2022 (**D**) (image: D. McWethy).

Increases in fire activity at the SFP during the early- and mid-Holocene, a period characterized by higher seasonality and warm summers, may foreshadow how recent warming could precondition the SFP watershed and surrounding forests for fire spread. Pronounced warm-season drying of peats and woody vegetation along with elevated temperatures that persist later into the autumn months will likely provide ample fuel drying to allow for larger fires across an expanded fire season. The rapid increase in thaw depression ponds since 2000 has led to almost complete drying of the fen peat matrix surrounding the collapse ponds, providing ample connected, dry fuels for fire spread. We expect that the thawing of the permafrost beneath the fen system, which has persisted throughout the Holocene, will result in the complete loss of the SFP permafrost feature within decades.

5. Conclusions

Despite its location in the high-alpine environment characterized by a short growing season and snowpack persisting through much of the year, high-severity fire activity was

recorded at the SFP in the early- and mid-Holocene under intensified seasonality (colder winters and warmer summers) and warmer fire-season conditions. Pronounced fluctuations in peat accumulation suggest mid-Holocene and late-Holocene conditions led to the degradation and loss of parts of the paleoenvironmental and paleofire records via erosive processes or consumption by fire. The paleofire record indicates high-severity fires occurred once every few hundred years during times when peat accumulation was consistent. This suggests that the climatic conditions associated with productive peat accumulation were also conducive to increased canopy cover and fire spread. Analysis of multiple proxies from the SFP sediments provides insights into our primary research questions.

- Stability of the SFP: The long-term paleoenvironmental record from the SFP suggests this low latitude fen palsa system experienced at least two periods of instability, when high seasonality and/or desiccation and possible increase in surface fires led to degredation of the fen palsa.
- Frequency and character of fire activity: High-severity fire activity was pronounced during the early- and mid-Holocene, whereas fire activity was likely obscured by partial loss of the sediment record during periods of instability of the SFP system. Desiccation and/or surface fires likely degraded or consumed portions of the peat surface, complicating the reconstruction of a complete fire and environmental record, as indicated by slow sedimentation rates, ca. 6000–8000 and 5000–0 cal yrs BP.
- Vegetation response to climate and fire: Vegetation was dominated by alpine conifers, sagebrush grasses and sedges and exhibited relatively stable response to climate variability and fire activity. Forest opening and increases in sagebrush and grasses were most evident during the high seasonality of the early- to mid-Holocene transition.
- Recent changes: Consistent with patterns observed in higher-latitude permafrost peatlands, recent decades of rapid warming have accelerated SFP degradation. Continued warming is likely to result in system collapse within decades. The loss of the SFP and change in the climate regime responsible for its formation will likely have far-reaching consequences for ecosystem dynamics, disturbance regimes, carbon storage and nutrient cycling in alpine environments throughout the Rocky Mountain cordillera.

Evaluation of the multiproxy paleoenvironmental record from the SFP site offers a rare, long-term perspective on alpine fire–climate interactions. High-severity fire activity was a common feature in this high-alpine watershed during the early- and mid-Holocene. Instability of the SFP system highlights the vulnerability of low-latitude permafrost sites to climate warming. Although the SFP represents a relatively rare feature in lower-latitude alpine settings, monitoring the rate and character of permafrost loss will be important for anticipating cascading effects of a warming climate on carbon storage, hydrology, fire activity, and ecological dynamics in high-alpine environments.

Supplementary Materials: The following supporting information can be downloaded at https://www.mdpi.com/article/10.3390/fire9030103/s1, Table S1: Radiocarbon dating information. Table S2: Macroscopic charcoal (>125 μm) raw data counts (pieces per cm^{-2}).

Author Contributions: Conceptualization, D.B.M. and M.A.; methodology, D.B.M. and M.A.; formal analysis, D.B.M. and M.A.; investigation, D.B.M. and M.A.; resources, D.B.M.; data analysis and curation, D.B.M., M.A. and A.T.-W.; writing—original draft preparation, D.B.M.; writing—review and editing, D.B.M., M.A. and A.T.-W.; visualization, D.B.M. and M.A.; funding acquisition, D.B.M. All authors have read and agreed to the published version of the manuscript.

Funding: This research was funded by NSF EAR 2149482 and NSF EAR 2503838 to D.B.M.

Institutional Review Board Statement: Not applicable.

Informed Consent Statement: Not applicable.

Data Availability Statement: Data supporting reported results can be found at NEOTOMA, https://www.neotomadb.org/ (accessed on 17 February 2026).

Acknowledgments: We thank John Wendt for field assistance. The authors have reviewed and edited the output and take full responsibility for the content of this publication.

Conflicts of Interest: The authors declare no conflicts of interest. The funders had no role in the design of the study; in the collection, analyses, or interpretation of data; in the writing of the manuscript; or in the decision to publish the results.

References

1. Pepin, N.; Bradley, R.S.; Diaz, H.F.; Baraer, M.; Caceres, E.B.; Forsythe, N.; Fowler, H.; Greenwood, G.; Hashmi, M.Z.; Liu, X.D.; et al. Elevation-dependent warming in mountain regions of the world. *Nat. Clim. Change* **2015**, *5*, 424–430. [CrossRef]
2. Minder, J.R.; Letcher, T.W.; Liu, C. The Character and Causes of Elevation-Dependent Warming in High-Resolution Simulations of Rocky Mountain Climate Change. *J. Clim.* **2018**, *31*, 2093–2113. [CrossRef]
3. Andrus, R.A.; Harvey, B.J.; Rodman, K.C.; Hart, S.J.; Veblen, T.T. Moisture availability limits subalpine tree establishment. *Ecology* **2018**, *99*, 567–575. [CrossRef]
4. Lenoir, J.; Gégout, J.C.; Marquet, P.A.; de Ruffray, P.; Brisse, H. A Significant Upward Shift in Plant Species Optimum Elevation During the 20th Century. *Science* **2008**, *320*, 1768–1771. [CrossRef]
5. Quadri, P.; Silva, L.C.R.; Zavaleta, E.S. Climate-induced reversal of tree growth patterns at a tropical treeline. *Sci. Adv.* **2021**, *7*, eabb7572. [CrossRef]
6. Pederson, G.T.; Stahle, D.; McWethy, D.B.; Toohey, M.; Jungclaus, J.; Lee, C.; Martin, J.; Alt, M.; Kichas, N.; Chellman, N.; et al. Dynamic treeline and cryosphere response to pronounced mid-Holocene climatic variability in the US Rocky Mountains. *Proc. Natl. Acad. Sci. USA* **2025**, *122*, e2412162121. [CrossRef]
7. Alt, M.; Puseman, K.; Lee, C.M.; Pederson, G.T.; McConnell, J.R.; Chellman, N.J.; McWethy, D.B. Organic layers preserved in ice patches: A new record of Holocene environmental change on the Beartooth Plateau, USA. *Holocene* **2023**, *34*, 338–352. [CrossRef]
8. Rehm, E.; Feeley, K.J. Many species risk mountain top extinction long before they reach the top. *Front. Biogeogr.* **2016**, *8*, e27788. [CrossRef]
9. Kichas, N.E.; Pederson, G.T.; Hood, S.M.; Everett, R.G.; McWethy, D.B. Increased whitebark pine (*Pinus albicaulis*) growth and defense under a warmer and regionally drier climate. *Front. For. Glob. Change* **2023**, *6*, 1089138. [CrossRef]
10. Krause, T.R.; Lu, Y.; Whitlock, C.; Fritz, S.C.; Pierce, K.L. Patterns of terrestrial and limnologic development in the northern Greater Yellowstone Ecosystem (USA) during the late-glacial/early-Holocene transition. *Palaeogeogr. Palaeoclimatol. Palaeoecol.* **2015**, *422*, 46–56. [CrossRef]
11. Krause, T.R.; Whitlock, C. Climate and vegetation change during the late-glacial/early-Holocene transition inferred from multiple proxy records from Blacktail Pond, Yellowstone National Park, USA. *Quat. Res.* **2013**, *79*, 391–402. [CrossRef]
12. Huerta, M.A.; Whitlock, C.; Yale, J. Holocene vegetation–fire–climate linkages in northern Yellowstone National Park, USA. *Palaeogeogr. Palaeoclimatol. Palaeoecol.* **2009**, *271*, 170–181. [CrossRef]
13. Whitlock, C. Postglacial Vegetation and Climate of Grand Teton and Southern Yellowstone National Parks. *Ecol. Monogr.* **1993**, *63*, 173–198. [CrossRef]
14. Whitlock, C.; Dean, W.E.; Fritz, S.C.; Stevens, L.R.; Stone, J.R.; Power, M.J.; Rosenbaum, J.R.; Pierce, K.L.; Bracht-Flyr, B.B. Holocene seasonal variability inferred from multiple proxy records from Crevice Lake, Yellowstone National Park, USA. *Palaeogeogr. Palaeoclimatol. Palaeoecol.* **2012**, *331–332*, 90–103. [CrossRef]
15. Iglesias, V.; Whitlock, C.; Krause, T.R.; Baker, R.G. Past vegetation dynamics in the Yellowstone region highlight the vulnerability of mountain systems to climate change. *J. Biogeogr.* **2018**, *45*, 1768–1780. [CrossRef]
16. Rust, R.A.; Minckley, T.A. Fire and hydrologically mediated diversity change in subalpine forests through the Holocene. *J. Veg. Sci.* **2020**, *31*, 380–391. [CrossRef]
17. Péwé, T.L. Alpine Permafrost in the Contiguous United States: A Review. *Arct. Alp. Res.* **1983**, *15*, 145–156. [CrossRef] [PubMed]
18. Fewster, R.E.; Morris, P.J.; Swindles, G.T.; Gregoire, L.J.; Ivanovic, R.F.; Valdes, P.J.; Mullan, D. Drivers of Holocene palsa distribution in North America. *Quat. Sci. Rev.* **2020**, *240*, 106337. [CrossRef]
19. Collins, E.I.; Lichvar, R.W.; Evert, E.F. Description of the only known fen-palsa in the contiquous United States. *Arct. Alp. Res.* **1984**, *16*, 255–258. [CrossRef]
20. Leppiniemi, O.; Karjalainen, O.; Aalto, J.; Luoto, M.; Hjort, J. Environmental Drivers of Palsa and Peat Plateau Occurrences: A Regional Comparison Across the Northern Hemisphere. *Permafr. Periglac. Process.* **2025**, *36*, 37–50. [CrossRef]

21. Zhang, Y.; Wolfe, S.A.; Morse, P.D.; Olthof, I.; Fraser, R.H. Spatiotemporal impacts of wildfire and climate warming on permafrost across a subarctic region, Canada. *J. Geophys. Res. Earth Surf.* **2015**, *120*, 2338–2356. [CrossRef]
22. Schulze, C.; Sonnentag, O.; Emmerton, C.A.; Harris, L.; Alcock, H.; Marouelli, K.; Hould Gosselin, G.; Knox, S.H.; Howard, R.; Skeeter, J.; et al. Large Carbon Losses from Burned Permafrost Peatlands During Post-Fire Succession. *Geophys. Res. Lett.* **2025**, *52*, e2025GL118344. [CrossRef]
23. Li, X.-Y.; Jin, H.-J.; Wang, H.-W.; Marchenko, S.S.; Shan, W.; Luo, D.-L.; He, R.-X.; Spektor, V.; Huang, Y.-D.; Li, X.-Y.; et al. Influences of forest fires on the permafrost environment: A review. *Adv. Clim. Change Res.* **2021**, *12*, 48–65. [CrossRef]
24. French, H.M. *The Periglacial Environment*; John Wiley & Sons: Hoboken, NJ, USA, 2018.
25. Schädel, C.; Gasser, T.; Rogers, B.M.; Treharne, R.; Turetsky, M.R.; Smith, T.; MacDonald, E.; Natali, S.M. Permafrost and wildfire carbon emissions indicate need for additional action to keep Paris Agreement temperature goals within reach. *Commun. Earth Environ.* **2026**. [CrossRef]
26. Pierce, W.G. Permafrost and thaw depressions in a peat deposit in the Beartooth Mountains, northwestern Wyoming. *Short Pap. Geol. Hydrol. Sci.* **1961**, *424*, 154–156.
27. Heidel, B.; Fertig, W.; Mellmann-Brown, S.; Houston, K.E.; Dwire, K.A. *Fens and Their Rare Plants in the Beartooth Mountains, Shoshone National Forest, Wyoming*; U.S. Department of Agriculture: Fort Collins, CO, USA, 2017; 110p.
28. Wise, E.K.; Woodhouse, C.A.; McCabe, G.J.; Pederson, G.T.; St-Jacques, J.-M. Hydroclimatology of the Missouri River Basin. *J. Hydrometeorol.* **2018**, *19*, 161–182. [CrossRef]
29. Whitlock, C.; Bartlein, P.J. Spatial Variations of Holocene Climatic-Change in the Yellowstone Region. *Quat. Res.* **1993**, *39*, 231–238. [CrossRef]
30. Stuiver, M.; Reimer, P.J. Extended ^{14}C database and revised CALIB radiocarbon calibration program. *Radiocarbon* **1993**, *35*, 92–98. [CrossRef]
31. Blaauw, M.; Christen, J.A. Flexible paleoclimate age-depth models using an autoregressive gamma process. *Bayesian Anal.* **2011**, *6*, 457–474. [CrossRef]
32. Bennett, K.D.; Willis, K.J. Pollen. Tracking Environmental Change Using Lake Sediments. In *Terrestrial, Algal, and Siliceous Indicators*; Smol, J.P., Birks, H.J.B., Last, W.M., Eds.; Kluwer Academic Publishers: Dordrecht, The Netherlands, 2002; Volume 3, pp. 5–32.
33. Faegri, K.; Iversen, J. *Textbook of Pollen Analysis*; Hafner Press: Copenhagen, Denmark, 1975; p. 295.
34. Kapp, R.O.; Davis, O.K.; King, J.E. *Pollen and Spores*, 2nd ed.; American Association of Stratigraphic Palynologists Foundation: Dallas, TX, USA, 2000.
35. McAndrews, J.H.; Berti, A.A.; Norris, G.N. *Key to Quaternary Pollen and Spores of the Great Lakes Region*; Royal Ontario Museum (ROM) Life Sciences Division: Toronto, ON, Canada, 1973.
36. Grimm, E.C. CONISS: A FORTRAN 77 program for stratigraphically constrained cluster analysis by the method of incremental sum of squares. *Comput. Geosci.* **1987**, *13*, 13–35. [CrossRef]
37. Whitlock, C.; Larsen, C. Charcoal as a Fire Proxy. In *Tracking Environmental Change Using Lake Sediments: Terrestrial, Algal, and Siliceous Indicators*; Smol, J.P., Birks, H.J.B., Last, W.M., Bradley, R.S., Alverson, K., Eds.; Springer: Dordrecht, The Netherlands, 2001; pp. 75–97.
38. Higuera, P.E.; Gavin, D.G.; Bartlein, P.J.; Hallett, D.J. Peak detection in sediment–charcoal records: Impacts of alternative data analysis methods on fire-history interpretations. *Int. J. Wildland Fire* **2010**, *19*, 996–1014. [CrossRef]
39. Higuera, P.E.; Brubaker, L.B.; Anderson, P.M.; Hu, F.S.; Brown, T.A. Vegetation mediated the impacts of postglacial climate change on fire regimes in the south-central Brooks Range, Alaska. *Ecol. Monogr.* **2009**, *79*, 201–219. [CrossRef]
40. Chellman, N.J.; Pederson, G.T.; Lee, C.M.; McWethy, D.B.; Puseman, K.; Stone, J.R.; Brown, S.R.; McConnell, J.R. High elevation ice patch documents Holocene climate variability in the northern Rocky Mountains. *Quat. Sci. Adv.* **2021**, *3*, 100021. [CrossRef]
41. Shuman, B.N.; Serravezza, M. Patterns of hydroclimatic change in the Rocky Mountains and surrounding regions since the last glacial maximum. *Quat. Sci. Rev.* **2017**, *173*, 58–77. [CrossRef]
42. Shuman, B.; Pribyl, P.; Minckley, T.A.; Shinker, J.J. Rapid hydrologic shifts and prolonged droughts in Rocky Mountain headwaters during the Holocene. *Geophys. Res. Lett.* **2010**, *37*, L06701. [CrossRef]
43. Shuman, B.; Henderson, A.K.; Colman, S.M.; Stone, J.R.; Fritz, S.C.; Stevens, L.R.; Power, M.J.; Whitlock, C. Holocene lake-level trends in the Rocky Mountains, USA. *Quat. Sci. Rev.* **2009**, *28*, 1861–1879. [CrossRef]
44. Parks, S.A.; Hefty, K.L.; Rushing, J.F.; Goeking, S.A.; Tomback, D.F.; Hood, S.M.; Toney, J.C.; Harrell, D.L.; Lindstrom, J.; Naficy, C.E.; et al. Whitebark pine in the United States projected to experience an 80% reduction in climatically suitable area by the mid-21st century. *Environ. Res. Lett.* **2025**, *20*, 104012. [CrossRef]

45. Munroe, J.S.; Crocker, T.A.; Giesche, A.M.; Rahlson, L.E.; Duran, L.T.; Bigl, M.F.; Laabs, B.J.C. A lacustrine-based Neoglacial record for Glacier National Park, Montana, USA. *Quat. Sci. Rev.* **2012**, *53*, 39–54. [CrossRef]
46. Cook, E.R.; Seager, R.; Heim, R.R., Jr.; Vose, R.S.; Herweijer, C.; Woodhouse, C. Megadroughts in North America: Placing IPCC projections of hydroclimatic change in a long-term palaeoclimate context. *J. Quat. Sci.* **2010**, *25*, 48–61. [CrossRef]

Disclaimer/Publisher's Note: The statements, opinions and data contained in all publications are solely those of the individual author(s) and contributor(s) and not of MDPI and/or the editor(s). MDPI and/or the editor(s) disclaim responsibility for any injury to people or property resulting from any ideas, methods, instructions or products referred to in the content.